

Supercontinuum generation with optical vortices

Dragomir N. Neshev¹, Alexander Dreischuh^{1,2},
Georgi Maleshkov², Marek Samoc³, and Yuri S. Kivshar¹

¹*Nonlinear Physics Centre, Research School of Physics and Engineering,
Australian National University, Canberra, Australia*

²*Department of Quantum Electronics, Faculty of Physics, Sofia University, Sofia, Bulgaria*

³*Institute of Physical and Theoretical Chemistry, Wrocław University of Technology, Wrocław,
Poland*

Abstract: We report on the generation of femtosecond supercontinuum in a solid state medium by an optical vortex beam. We show that the continuum generation process is initiated by the filamentation of the vortex, resulting in a spatially divergent continuum.

© 2010 Optical Society of America

OCIS codes: (190.4420) Nonlinear optics, transverse effects in; (260.6042) Singular optics

References and links

1. J. M. Dudley, G. Genty, and S. Coen, "Supercontinuum generation in photonic crystal fiber," *Rev. Mod. Phys.* **78**, 1135–1184 (2006).
 2. R. R. Alfano and S. L. Shapiro, "Emission in the region 4000 to 7000 Å via four-photon coupling in glass," *Phys. Rev. Lett.* **24**, 584–587 (1970).
 3. M. Bellini and T. W. Hänsch, "Phase-locked white-light continuum pulses: toward a universal optical frequency-comb synthesizer," *Opt. Lett.* **25**, 1049–1051 (2000).
 4. H. I. Sztul, V. Kartazayev, and R. R. Alfano, "Laguerre-Gaussian supercontinuum," *Opt. Lett.* **31**, 2725 (2006).
 5. D. G. Grier, "A revolution in optical manipulation," *Nature* **424**, 810–816 (2003).
 6. G. Foo, D. M. Palacios, and G. A. Swartzlander, Jr., "Optical vortex coronagraph," *Opt. Lett.* **30**, 3308–3310 (2005).
 7. S. Furfapter, A. Jesacher, S. Bernet, and M. Ritsch Marte, "Spiral interferometry," *Opt. Lett.* **30**, 1953–1955 (2005).
 8. G. Molina Terriza, J. P. Torres, and L. Torner, "Twisted photons," *Nature Physics* **3**, 305–310 (2007).
 9. T. F. Scott, B. A. Kowalski, A. C. Sullivan, C. N. Bowman, and R. R. McLeod, "Two-color single-photon photoinitiation and photoinhibition for subdiffraction photolithography," *Science* **324**, 913 (2009).
 10. A. V. Gorbach and D. V. Skryabin, "Cascaded generation of multiply charged optical vortices and spatiotemporal helical beams in a Raman medium," *Phys. Rev. Lett.* **98**, 243601 (2007).
 11. A. Berzanskis, A. Matijosius, A. Piskarskas, V. Smilgevicius, A. Stabinis, "Conversion of topological charge of optical vortices in a parametric frequency converter," *Opt. Commun.* **140**, 273–276 (1997).
 12. W. J. Firth and D. V. Skryabin, "Optical solitons carrying orbital angular momentum," *Phys. Rev. Lett.* **79**, 2450 (1997).
 13. V. Tikhonenko, J. Christou, and B. Luther-Davies, "Spiraling bright spatial solitons formed by the breakup of an optical vortex in a saturable self-focusing medium," *J. Opt. Soc. Am. B* **12**, 2046–2052 (1995).
 14. L. T. Vuong, T. D. Grow, A. Ishaaya, A. L. Gaeta, G. W. 't Hooft, E. R. Eliel, and G. Fibich, "Collapse of optical vortices," *Phys. Rev. Lett.* **96**, 13390 (2006).
 15. A. Brodeur and S. L. Chin, "Ultrafast white-light continuum generation and self-focusing in transparent condensed media," *J. Opt. Soc. Am. B* **16**, 637–650 (1999).
 16. A. Vinçotte and L. Bergé, "Femtosecond optical vortices in air," *Phys. Rev. Lett.* **95**, 193901 (2005).
 17. I. Buchvarov, A. Trifonov, and T. Fiebig, "Toward an understanding of white-light generation in cubic media-polarization properties across the entire spectral range," *Opt. Lett.* **32**, 1539–1541 (2007).
 18. D. Rozas, C. T. Law, and G. A. Swartzlander, Jr., "Propagation dynamics of optical vortices," *J. Opt. Soc. Am. B* **14**, 3054–3065 (1997).
-

The generation of supercontinuum (SC) light with ultra-short laser pulses is one of the most fascinating nonlinear phenomena in optics [1]. Such broadband or white-light supercontinuum finds numerous applications in frequency metrology, spectroscopy, and optical coherence tomography. First observed in bulk glasses in early 70's [2], the interest towards this effect has been renewed with the development of the photonic crystal fibres [1]. While in fibres, the supercontinuum spatial profile is governed by the mode structure of the fibre, in bulk materials no mode selection is present and the spatial structure of the generated continuum can be determined by the spatial mode of the fundamental laser pulse. Importantly, this opens the possibility for generation of supercontinuum light with complex spatial structure [3], including supercontinuum optical vortices. Despite the recent proposals of such generation [4], no supercontinuum generation with beams of complex spatial and phase structure has been studied experimentally.

In this work we report on the first to our knowledge, experimental studies of generation of supercontinuum light by optical vortices (OVs) – beams containing spiral phase along their azimuthal coordinate. We use short femtosecond pulses with an embedded vortex phase singularity and focus them into a solid state medium where self-focusing and four-wave mixing induce spectral broadening and generation of broad supercontinuum. Our results demonstrate that the supercontinuum is driven by a filamentation process of the OV where each filament triggers independent continuum generation. We show that due to the intrinsic intensity noise in the OV beam profile, the supercontinua generated from the different filaments are not coherently added into the output supercontinuum beam and therefore the vortex phase information is not transferred to the white-light continuum. As such, the generated white light appears in the far-field as a broad background surrounding the fundamental OV. Our studies suggest that direct generation of coherent white light optical vortex beam is not possible, unless special effort is paid in order to suppress the noise in the filamentation process.

The OVs are associated with the presence of a spiral phase dislocation in the wavefront of a light beam that determines its phase and intensity structure. The study of OVs has received a special attention in recent years due to a variety of potential applications including particle micro-manipulation [5], imaging [6], interferometry [7], quantum information [8] and most recently high-resolution microscopy and lithography [9]. In the latter, optical vortices of different wavelengths are used to de-excite (bleach) the molecules of the material, enabling the detection or creation of sub-diffraction resolution features. Obviously, in such applications, OVs at various wavelengths or even multi-color OVs are desirable.

Multi-colored OVs can be created through nonlinear frequency conversion processes, such as four-wave mixing (FWM). Unlike OV propagation in a Raman [10] or quadratic nonlinear medium [11], the FWM process preserves the topological charge of the OVs and can be expected to be an important factor for white-light vortex generation. However, as the FWM process always exists together with beam self-focusing, special consideration about the vortex integrity needs to be taken into account. The OV dynamics in a nonlinear medium is well known to lead to vortex break-up or disintegration. Predicted in [12] and observed in [13, 14] such vortex break-up is an important issue for white-light or supercontinuum generation.

To experimentally analyze the structure of a supercontinuum beam generated by an optical vortex we focus 150 fs pulses (peak power of 15 MW, central wavelength 775 nm) from a chirped-pulse amplification system (CPA-2001, 250 Hz, Clark-MXR Inc.) into a bulk material. Various materials, including BK7 glass, quartz, and water have been tested, however the best results (thermal stability and SC bandwidth) have been achieved with a 5 mm thick sample of CaF_2 (material bandgap, $E_{\text{gap}} = 10.2$ eV) [15]. For optical vortex generation, we use a computer generated hologram (CGH), fabricated by etching of a vortex interference pattern onto a glass substrate. The efficiency of the hologram is 30%, and the large grating period of $80\mu\text{m}$ assures negligible chromatic dispersion over the pulse bandwidth.

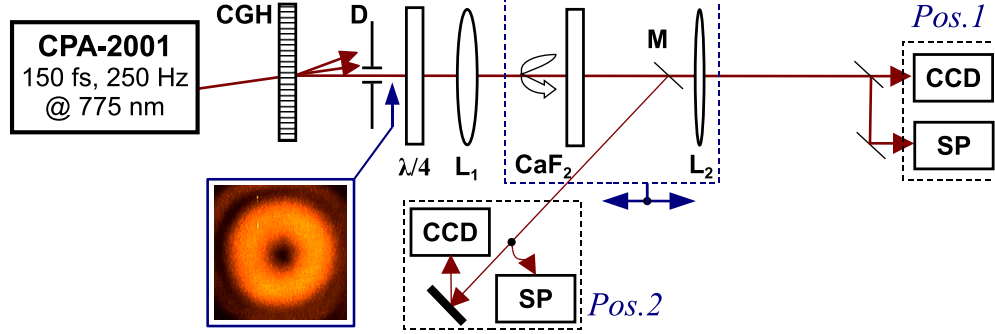


Fig. 1. Experimental setup: CPA-2001 – femtosecond laser and chirped pulse amplifier (Clark-MXR); CGH – computer generated hologram; D – diaphragm; $\lambda/4$ – quarter waveplate; L_1 – focusing lens of a focal length $f = 30$ cm; L_2 – imaging lens of $f = 10$ cm; CaF_2 – 5 mm thick rotating sample, which longitudinal position is varied simultaneously with the mirror M and the lens L_2 ; CCD – color camera; SP – spectrometer (Avantes). *Pos. 1* and *Pos. 2* denote data acquisition in the near- and far-field, respectively. Inset – typical vortex profile observed after the CGH.

The experimental setup is shown in Fig. 1. An iris diaphragm D , located about 100 cm behind the CGH and 200 cm in front of the focusing lens L_1 is used to select the first diffraction order of the hologram. This diffraction order contains the encoded OV (see inset in Fig. 1). The input beam polarization (linear or circular) is controlled by a $\lambda/4$ waveplate. The CaF_2 sample is continuously rotated to avoid its possible damage due to thermal effects.

In order to smoothly control the vortex beam intensity inside the CaF_2 sample, we vary the position of the beam waist with respect to the sample, keeping the sample-to-imaging lens distance unchanged. Loose focusing by the lens L_1 ($f = 30$ cm) is sufficient to observe strong supercontinuum generation. The data acquisition system consist of a color charge-coupled device (CCD) camera and a fiber-optic spectrometer (SP, Avantes). Our experimental setup allows for simultaneous measurements of the near- and far-field intensity profiles. The near field is recorder through the imaging lens L_2 at position *Pos. 1*). The far-field intensity distribution is observed on a screen (*Pos. 2*), located ~ 190 cm away from the flip-mirror M and mounted on the same translation stage as the rotating sample.

First we measure the broadening of the beam spectrum with increasing beam intensity when we shift the beam focus closer to the CaF_2 sample. All of the generated white-light is coupled into the fibre spectrometer and the measurements are performed for different offsets of the beam focus. The obtained results are depicted in Fig. 2(a) as a combined plot of the normalized spectra versus beam-focus offset. At large offsets (3 – 1 mm), we only see spectral broadening of the main part of the laser spectrum near the carrier wavelength of 775 nm due to self-phase modulation. Above a certain intensity threshold, however new frequency components are being generated, predominantly in the shorter-wavelength spectral range. At zero offset (beam waist approximately coinciding with the center of the CaF_2 crystal), we observe strong supercontinuum generation in the spectral range of 450 – 900 nm.

While the spectral broadening in the process of supercontinuum generation shows great similarities with the earlier studies using Gaussian beams, the observed spatial mode profiles are quite different. Three mode profiles are shown in Figs. 2(b-d) for focus-to-sample offset of 0, 0.75, and 2.5 mm, respectively. In these far-field images, the original vortex beam appears as a small bright dot in the center [see Fig. 2(b)]. However, above the SC generation threshold, we see that the generated white-light beams experiences much larger divergence than the original

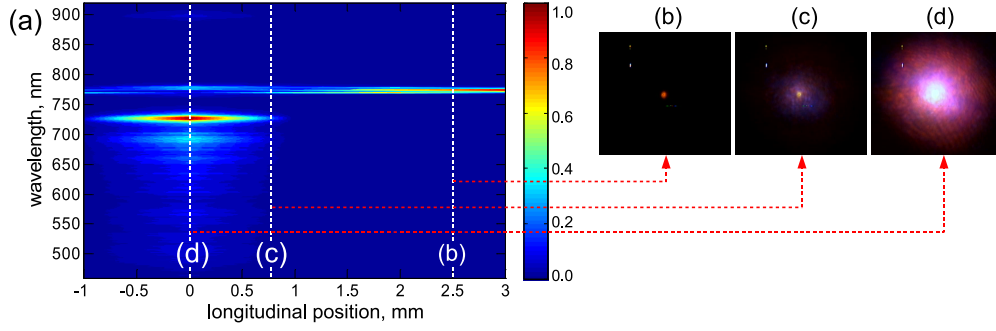


Fig. 2. Supercontinuum generation from a vortex beam. (a) Normalized spectrum of the output light for different positions of the beam waist with respect to the CaF_2 sample. (b-d) Color far-field profiles for different input positions of the beam waist.

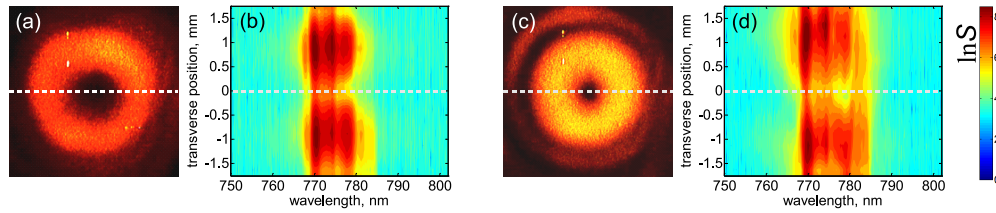


Fig. 3. Far-field vortex intensity profiles in the spectral range 750 – 800 nm at longitudinal positions (a) 3 mm and (c) 0 mm. (b, d) The corresponding spectral content (log scale - $\ln S$) of the vortex core recorded at 16 positions along the dashed line in (a, c).

OV beam. This simple observation suggest that the SC is not a coherent superposition of all parts of the vortex. This fact is also confirmed by the lack of zero intensity in the center of the supercontinuum beam [Fig. 2(d)].

In order to closely examine the process of supercontinuum generation from the vortex beam, we measure only the spectral content of the central part of the beam, constituting the original OV in the far-field (*Pos. 2* in Fig. 1). In Fig. 3(a, c) we show the OV image in the far-field for two different offsets of 3 and 0 mm, respectively. In both cases we observe a well preserved vortex profile, suggesting that the OV survives the vortex break-up previously observed in bulk-glasses [14]. We only see that at high beam intensities (position zero) the laser pulses have accumulated about 30% spectral broadening due to self-phase modulation. This is depicted in Fig. 3(b, d) showing the log-scale of the spectral content in the range 750 – 800 nm. The spectrograms in Fig. 3(b, d) are obtained by superimposing individual spectra taken at 16 different positions along a horizontal line, passing through the OV origin, as indicated with a dashed line in Fig. 3(a, c). The vortex beam bandwidth, however, is substantially smaller than this of the SC itself. The conclusion of this observation is that the coherent fraction of the continuum is weak and the observed strong supercontinuum generation is not driven by the OV as a whole, but is most likely a superposition from independent parts of the OV beam.

It is also worth mentioning that at the initial stage of the SC generation, for average laser powers slightly exceeding 8 mW, we can observe colored interference fringes. Such fringes are seen in the blue part of the spectrum, as shown in Fig. 4(a,b). Fig. 4(a) shows the full colour image of all spectral components, while Fig. 4(b) depicts the extracted blue frequency components only, in order to enhance the visibility of the interference fringes. Triangular and square lattices of fringes have also been observed, however they could not be clearly recorded. We attribute

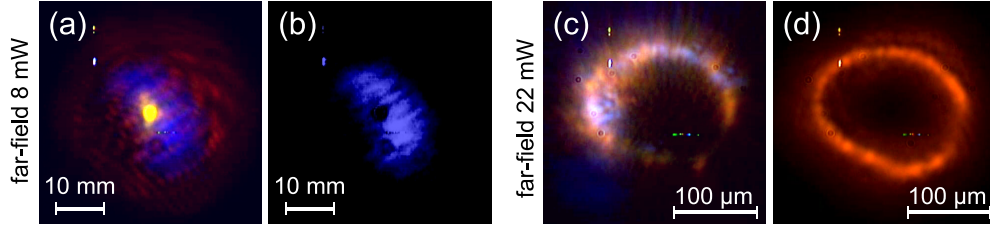


Fig. 4. (a,b) Far-field intensity profile of the supercontinuum at 8 mW average laser power, showing fringes in the blue spectral range. (a) Full color profile, (b) only the blue components have been extracted from (a) to improve fringe visibility. (c,d) Near-field intensity profile of the supercontinuum radiation at the back side of the CaF_2 sample at 22 mW average laser power, showing the formation of light filaments and their contribution to the supercontinuum generation. (c) Full-colour image and (d) image filtered with a long-pass spectral filter.

these interference structures to the coherent superposition of supercontinua generated from different (but low in number) light filaments. The general observations show that the brighter the SC, the lower the visibility of these interference structures is.

To analyze the origin of the SC generation and the preservation of the vortex profile in the far-field, we image the output beam profile onto a CCD camera - *Pos. 1*. In Fig. 4(c) we show the color image of the light intensity profile at average laser power of 22 mW and zero offset of the beam focus with respect to the sample. From this image, we can conclude that the white-light is being generated independently from various different places along the vortex ring. Obviously, these places are determined by self-focusing and filament formation, similar to the process of optical vortex filamentation in air [16]. To clarify this effect, we filter-out all newly generated spectral components using a dielectric laser mirror M (Fig. 1) and monitor only the wavelengths of the fundamental laser beam. In the obtained image [Fig. 4(d)] it is seen that a large number of hot spots is being formed around the vortex ring. At the position of these hot spots the intensity exceeds the threshold for supercontinuum generation and they became the sources of white light. However, their mutual coherence is compromised due to the intrinsic noise on the OV beam and the modulation instability.

Additional measurements performed with circular polarization at 22 mW show qualitatively the same behavior, however with slightly improved circular symmetry of the filaments in comparison to the case shown in Fig. 4(d). The threshold for supercontinuum generation with circular polarization is also increased, as observed in earlier works [17].

We further study the process of OV filamentation, which is important for understanding of the supercontinuum generation with a complex-phase fundamental beam. For this purpose we monitor the near-field OV intensity profile at the fundamental wavelength using a notch filter. The profiles are recorded at several different offsets of the beam waist with respect to the sample. In Fig. 5 we show a comparison between low power (22 μW - left column) and high power (22 mW - right column) of the input OV beam.

In the linear images (top), it is seen that the OV decreases its size with decreasing the focusing lens-to-sample distance, while its circular symmetry is being preserved. In the nonlinear regime (bottom), the OV experiences self-focusing which is accompanied by distortion of the circular symmetry and formation of an increasing number of hot spots [from (a) to (e)]. These hot spots are the sources of SC radiation, but have a much smaller size than the original OV beam and therefore the generated SC diffracts much stronger than the fundamental OV beam. Because of this much higher diffraction, the SC appears in the far field as a wide background for the fundamental OV. As could be expected, the hot spots appear arranged along the vortex ring, i.e.

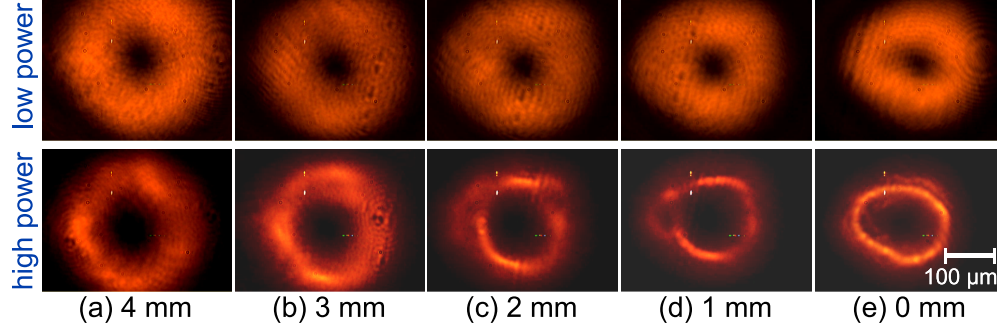


Fig. 5. Near-field OV profiles observed for low (top) and high (bottom) power at focusing lens-to-sample distance of 4, 3, 2, 1, 0 mm, respectively. At high average power of 22 mW (bottom row) the vortex ring experiences strong self-focusing and hot spot formation.

at positions of the highest local intensity. The exact place of each hot spot however is dictated by the modulation instability of the vortex, driven by the intrinsic intensity noise on the beam. Note that despite the hot spots, in all frames the OV core remains well preserved. This is due to the fact that the vortex instability can not fully develop in the short nonlinear crystal.

In conclusion, we have reported on the first experimental demonstration of femtosecond supercontinuum generation by an optical vortex beam. Our results demonstrate that the initial spatial profile of an optical vortex is well preserved in the process of supercontinuum generation. However, the generated continuum appears as a wide white-light background surrounding the fundamental optical vortex. We have deduced that strong diffraction of the supercontinuum generated from each filament is the reason for the observed wide white-light background. Depending on the initial beam intensity, the continua generated from a low number of filaments can interfere, resulting in pronounced interference fringes for certain spectral components. However, when a large number of filaments are involved in the supercontinuum generation process the phase of the vortex beam is not transferred into the supercontinuum spatial profile, due to the initial noise on the OV profile.

We acknowledge the support by the Australian Research Council, the National Science Foundation, Bulgaria (project DO-02-0114/2008), and by the Sofia University Science Fund (project 128/2009). We thank W. Krolikowski, D. Skryabin, and I. Buchvarov for the useful discussions.